Am J Transl Res 2016;8(3):1379-1396
www.ajtr.org /ISSN:1943-8141/AJTR0022584

Original Article

Fabrication and clinical application of easy-to-operate pre-cured CPC/rhBMP-2 micro-scaffolds for bone regeneration

Dan Lin[1,2,3], Jing Zhang[1,3], Feng Bai[5], Xuehua Cao[1,2], Cunyi Fan[6], Yuan Yuan[1,2,3], Jinwu Wang[4], Jian Zhang[7], Changsheng Liu[1,2,3]

[1]The State Key Laboratory of Bioreactor Engineering, East China University of Science and Technology, Shanghai 200237, P.R. China; [2]Key Laboratory for Ultrafine Materials of Ministry of Education, East China University of Science and Technology, Shanghai 200237, P.R. China; [3]Engineering Research Center for Biomedical Materials of Ministry of Education, East China University of Science and Technology, Shanghai 200237, P.R. China; [4]Department of Orthopaedic Surgery, Ninth People's Hospital of Shanghai Jiao Tong University, Shanghai 200011, P.R. China; [5]Department of Orthopedics in 451st Military Hospital, Shaanxi, Xi'an 710054, P.R. China; [6]Sixth People's Hospital of Shanghai Jiao Tong University, Shanghai 200233, P.R. China; [7]Zhongshan Hospital of Shanghai, Shanghai 200032, P.R. China

Received December 23, 2015; Accepted January 18, 2016; Epub March 15, 2016; Published March 30, 2016

Abstract: Bone tissue engineering scaffolds loading growth factors have been considered as the most perspective among all bone substitutes, yet little progress of its clinical translation has been made. The concept of "micro-scaffolds" was proposed in this study to provide a trajectory to the clinical translation of porous scaffolds. Combining CPC and rhBMP-2, a pre-cured CPC/rhBMP-2 micro-scaffold has been successfully developed and further applied as an easy-to-operate filler for bone regeneration in a pilot clinical study. The results demonstrated superior overall performances of CPC/rhBMP-2 microffolds to traditional therapies, with not only shortened repairing time and improved repairing qualities, but also the potential in treating fractures that are most challenging for current therapies. This pilot clinical study of CPC/rhBMP-2 microffolds further promoted the clinical translation of porous scaffolds for bone regeneration, and provided new insights for future development of artificial bone substitutes.

Keywords: CPC, rhBMP-2, bone regeneration, scaffolds

Introduction

Considerable bone defects resulting from non-union fractures, severe trauma, malignancy resection or infection, have raised great demands for clinical bone repair [1]. Large bone defects that cannot heal on its own require implantation of suitable bone grafts into the defect site [2]. Bone grafts include autografts, allografts and artificial bone substitutes. Autograft remains the gold standard in orthopaedic surgery due to its excellent osteoinductive and osteoconductive capability, yet limited tissue availability, donor site morbidity and additional surgical pain restrict their clinical applications [3, 4]. As a sub-optimal alternative, allografts have risks of immune rejection and disease transmission [5, 6]. These complications necessitate the pursuit of synthetic substitutes for treatment of these formidable defects [7].

Bone tissue engineering scaffolds have been widely developed and are considered as the most perspective among all bone substitutes. Macroporosities of scaffolds, comparing to dense materials, have been demonstrated as a prerequisite for bone formation *in vivo*. Based on previous studies [8, 9], the minimum requirement of pore size is considered to be ~100 μm for cell migration and nutritious transportation, and pore sizes > 300 μm are recommended, due to enhanced new bone formation and formation of capillaries. To date, researchers have developed various biomaterials into porous scaffolds, and some of them have been successfully applied in clinic, such as β-tricalcium phosphate (β-TCP) and biphasic calcium phosphate (HA/TCP) scaffolds [10-12]. However, a major problem of these artificial scaffolds is their deficient osteoinductivity compared to autografts, which might cause delayed union or

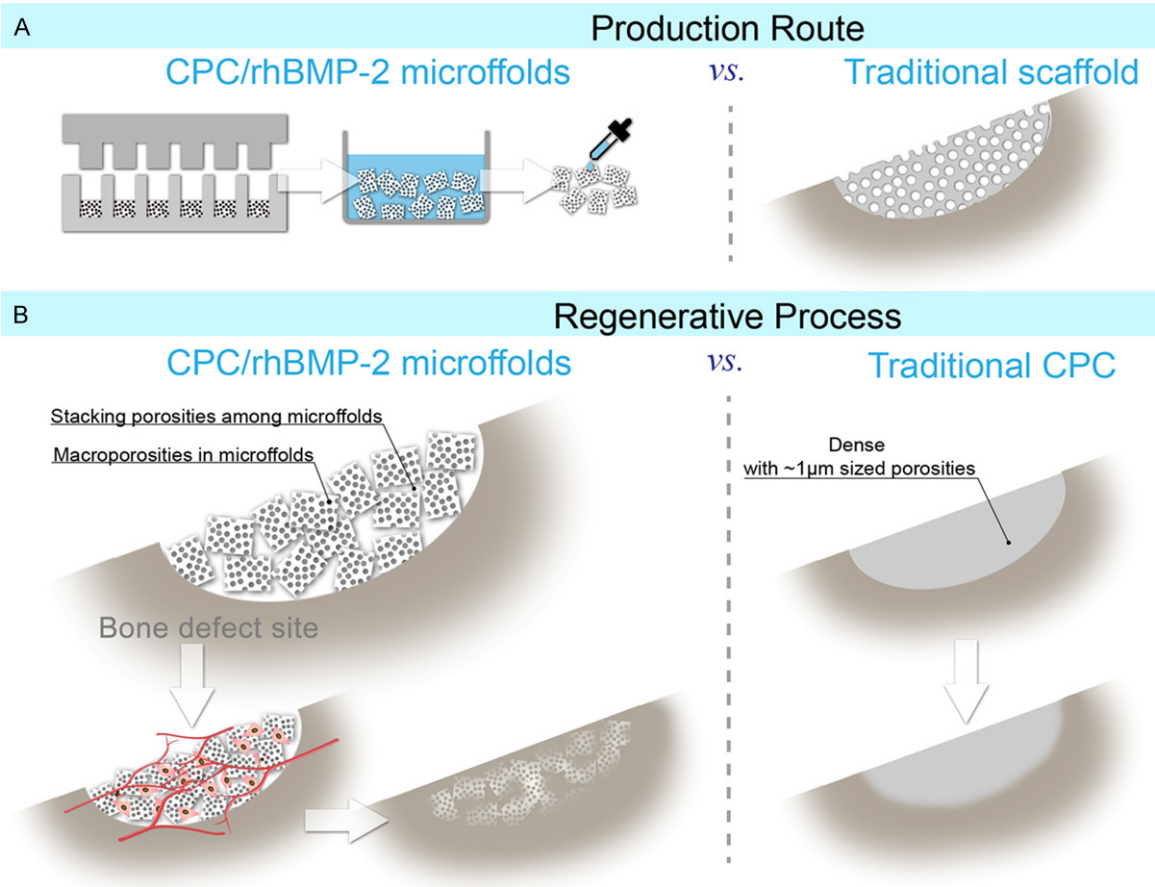

Scheme 1. Design of CPC/rhBMP-2 microffolds and comparison between microffolds and traditional scaffolds/traditional CPC. (A) Massive production route of CPC/rhBMP-2 microffolds: molding, salt leaching and rhBMP-2 immobilization. In comparison with traditional scaffolds: need of customization according to the defect size and shape, which is time-costing and requires specific equipment. (B) Rapid regeneration process by CPC/rhBMP-2 microffolds: abundant porosities allow cell ingrowth and vascularization, which renders rapid formation of new bone tissue and synchronous degradation of material. In comparison with traditional CPC paste: bioresorption layer by layer slowly due to its high density, and thus not being replaced by bone tissue until years later.

even nonunion in clinic [13, 14]. Another challenging problem that needs to be addressed in the clinical translational process is the customization of the scaffold according to the defect size and shape of the patient, which often requires a long period and is hard to achieve.

Currently, a widely efficient and clinically applicable way to promote endogenous repair mechanism and enhance bone formation is the loading of growth factors into biomaterials [15, 16]. Among all growth factors, bone morphogenetic protein-2 (BMP-2), a highly potent osteoinductive growth factor, has been considered as the most notable cytokine to enhance bone formation and bone tissue reconstruction [17, 18]. Recombinant human BMP-2 (rhBMP-2)-loaded absorbable collagen sponge has been approved by FDA in 2002 for interbody fusion surgeries, and its osteogenic capacity has been validated in numerous studies [19-21]. However, due to the lack of sustained release, low dosage of rhBMP-2 with desirable therapeutic efficacy remains a challenge in the therapy of bone defects [22, 23]. High dosage not only increases the potential risks associated with excessive concentrations of rhBMP-2, but also raises the therapeutic costs to an unaffordable level that hampers further applications of rhBMP-2 [24, 25]. Although researches have realized the sustained release of rhBMP-2 from different scaffolds, most of the BMP-2-loaded scaffolds are still confined to *in vitro* and animal experiments, and still have a long way from bench to bedside [26].

Calcium phosphate cement (CPC), a bioresorbable bone substitute, has been widely applied

in clinic due to its outstanding properties including similarity in composition to bone mineral, osteoconductivity, excellent bioactivity and cytocompatibility. The performances of CPC scaffolds *in vitro* and in animal models have been widely reported [27, 28]. Based on these situations and to address the aforementioned two major problems, by combining CPC and rhBMP-2, two mature clinical applications of material and growth factor, we have successfully developed a pre-cured CPC/rhBMP-2 micro-scaffold and further applied it as an easy-to-operate filler for bone regeneration in clinic. We proposed the concept of "microffolds" (short for "micro-scaffolds"), which can be massively produced in advance, and is easy to operate as bone filler during the surgery (**Scheme 1A**). The porous structure of microffold and the stacking macroporosities among the microffolds ensure rapid ingrowth of tissue and fast degradation of the material (**Scheme 1B**). Physicochemical properties and protein release kinetics of the microffolds were characterized. In a rabbit distal femur defect model, bone regeneration was achieved in 3 months after CPC/rhBMP-2 scaffold implantation, with regenerated tissue similar to normal tissue. A pilot clinical study was initiated in 81 patients to test safety and preliminary efficacy in humans (bone tissue repairing capacity) and to evaluate standard clinical and rehabilitation protocols that are not possible in animal models. Compared to traditional therapies by CPC paste, the average fracture healing time (for bony reunion) was 0.5~2 month shortened and the repairing qualities were improved by CPC/rhBMP-2 microffolds. This bench-to-bedside translation represents a potential development of the clinical treatment of bone defects.

Materials and methods

Preparation and characterization of CPC/rhBMP-2 microffolds

CPC powders and rhBMP-2 used in this study were both from Shanghai Rebone Biomaterials Co. Ltd. (Shanghai, China). The CPC powders were consisted of equimolar tetracalcium phosphate (TECP) and dicalcium phosphate anhydrous (DCPA).

The CPC microffolds were prepared through a salt leaching and molding method, with sodium chloride (NaCl) particles (size of ~500 μm) as macroporous porogen, and saturated NaCl solution as cement liquid and microporous porogen. Briefly, CPC powders, NaCl particles were mixed in a small amount of saturated NaCl solution to form a cement paste, which was cast into the mold with desirable shape (Ø 3 × 4 mm) under a pressure of 2 MPa for 1 min to prepare cylinder samples. After 3 days' curing at 37°C and 100% air humidity, the samples were soaked in purified water for 3 days (water renewed every 12 h) until the complete dissolution of NaCl, then dried at 100°C for 12 h to obtain the CPC microffolds.

After sterilization, a certain amount of rhBMP-2 solution was dropped onto CPC microffolds and evacuated for 30 min for fully adsorption of the protein into the microporosities. A dose of 1 mg/g (mg protein/g microffold) rhBMP-2 was applied. After lyophilized, the final CPC/rhBMP-2 microffolds were obtained. The CPC/rhBMP-2 microffolds could be long-term preserved at 4°C in sterile conditions before use.

The CPC/rhBMP-2 scaffolds used in animal experiments were prepared through a similar process, in which the shape and size of the mold was chosen according to the rabbit distal femur defect model (Ø 4.2 × 5 mm).

The phase composition of CPC was characterized by X-ray diffraction (XRD, Rigaku Co., Japan). The macroporous morphology and the microstructure of CPC microffolds were observed by scanning electron microscope (SEM, JSM-6360LV, JEOL).

In vitro release and bioactivity of rhBMP-2 from CPC/rhBMP-2 microffolds

The *in vitro* protein release was studied by suspending the CPC/rhBMP-2 microffolds in PBS (0.1 g scaffold/1 mL PBS) and maintaining it in a constant temperature incubator shaker (37°C, 100 rpm). At fixed time intervals, all release solutions were collected, and an identical volume of fresh PBS was added. RhBMP-2 concentration of each collected sample was measured by an ELISA kit to calculate the releasing amount. Secondary structures of free rhBMP-2 and the released rhBMP-2 were analyzed by circular dichroism (CD) measurements and estimated by CD spectra deconvolution software CDNN. Receptor-binding capacity and ALP activity were further assayed to evaluate

Table 1. Secondary structure content of free rhBMP-2 and microffold-released rhBMP-2 calculated by CDNN

	α-Helix	β-Parallel	β-Turn	Random Coil	Structural Change
Free rhBMP-2	9.60%	32.50%	15.70%	42.20%	-
Released rhBMP-2	8.20%	28.10%	12.80%	50.90%	5.69%

Table 2. Primer sequences used in real-time quantitative reserve transcription-polymerase chain reaction (RT-qPCR)

Primer	Sequences
ALP-for	CTCCGGATCCTGACAAAGAA
ALP-rev	ACGTGGGGGATGTAGTTCTG
Col I-for	CGTGACCAAAAACCAAAAGTGC
Col I-rev	GGGGTGGAGAAAGGAACAGAAA
OC-for	GCCCTGACTGCATTCTGCCTCT
OC-rev	TCACCACCTTACTGCCCTCCTG
Runx2-for	ATCCAGCCACCTTCACTTACACC
Runx2-rev	GGGACCATTGGGAACTGATAGG
β-actin-for	CACCCGCGAGTACAACCTTC
β-actin-rev	CCCATACCCACCATCACACC

the bioactivity of the released rhBMP-2, of which the detailed protocols are described as below.

To evaluate the receptor-binding capacity of the released rhBMP-2, rBMSCs were cultured with microffold-released rhBMP-2 and free rhBMP-2 respectively. After 4 h incubation, cells were fixed with 1% glutaraldehyde at 4°C for 15 min, then blocked with 1% BSA solution for 1 h at 37°C. After washed with PBS twice, cells were incubated with anti-BMP-2 antibody (R&D systems Inc., Minneapolis, USA) at 37°C for 1 h and 4°C for 1 h, then with FITC-conjugated goat-anti-mouse IgG (Sigma, St. Louis, USA) for 1 h at room temperature. 2-(4-Amidinophenyl)-6-indolecarbamidine dihydrochloride (DAPI, Beyotime Biotech, Jiangsu, China) solution was added to stain cell nucleus for 5 min. The amount of rhBMP-2 that bound to receptor on cell surface could be visualized using confocal laser-scanning microscopy (CLSM, Nikon A1R, Japan).

To evaluate the ALP activity of the released rhBMP-2, rBMSCs were cultured with microffold-released rhBMP-2 and free rhBMP-2 respectively. After 3 and 7 days of culture, the medium was removed and 200 μL Nonidet P-40 (NP-40, 1%) solution was added to each well. Samples were incubated for 1 h to obtain cell lysates. Then 50 μL of the cell lysates from each sample was pipetted to 96-well plates. 50 μL of 2 mg/mL p-nitrophenyl phosphate substrate solution (pNPP, Sangon, Shanghai, China) was added and incubated for 2 h at 37°C, the reaction was quenched by adding 100 μL NaOH (0.1 mol/L) and ALP activity was quantified by the absorbance at a wavelength of 405 nm using a microplate reader. Total protein content of each cell lysate was determined using a BCA protein assay kit. ALP levels were normalized with total protein content, and all experiments were performed in quadruplicates.

Evaluation of cell attachment and proliferation

For morphology observation of the cells attached on the microffold, rBMSCs were seeded on CPC/rhBMP-2 microffolds in 24-well culture plates at a density of 2×10^5 cells/well, and after 24 h incubation, samples were fixed with glutaraldehyde solution (2.5%) for 15 min. Then fixed cells were incubated with FITC-Phalloidin (5 μg/mL) and DAPI (5 μg/mL) for cytoskeleton and cellular nuclei staining, respectively. Cell morphologies were visualized using confocal laser-scanning microscopy (CLSM, Nikon A1R, Japan). Detailed rBMSCs morphology was further observed by SEM. After 12 h incubation, cells were fixed and dehydrated in ascending concentrations of ethanol (50, 70, 80, 90, 95 100, v/v%, 5 min at each gradient), followed by immersing in isoamyl acetate for 20 min and vacuum-dried at 37°C for 4 h.

Cytotoxicity and cell proliferation on the microffolds were evaluated by MTT assay, and a seeding density of 1×10^4 cells/well was applied. At each time point, 30 μL MTT solution (5 mg/mL) was added and incubated at 37°C for 4 h to allow formation of formazan crystals, which were subsequently dissolved with DMSO. Numbers of total cells in the plate well and of cells on the scaffold were quantified to evaluate toxicity, cell attachment and proliferation on the scaffolds respectively. The optical density (OD) value was measured at 492 nm using a microplate reader (SPECTRAmax 384, Molecular Devices, USA) to quantify the number of cells. Additional cultures without scaffolds were set as blank control.

Evaluation of osteogenic capacity in vitro

Osteogenic gene expression analyses were performed using Bio-Rad real-time quantitative

reserve transcription-polymerase chain reaction (RT-qPCR) system (Bio-Rad, Hercules, CA, USA). Osteogenic differentiation markers: ALP, type I collagen (Col I), osteocalcin (OC) and runt-related transcription factor 2 (Runx2) were evaluated, with β-actin gene used as housekeeping gene. Relative expression level for each gene (fold change) to that of CPC microffolds without rhBMP-2 was calculated. All experiments were performed in quadruplicates. Primer sequences used in this study were listed in **Table 2**.

Evaluation of osteogenic capacity in vivo: rabbit distal femur defect model

Eighteen 5-month-old New Zealand white rabbits (National Tissue Engineering Center, Shanghai, China) with an average weight of 3 kg were used and randomly divided into two groups: CPC and CPC/rhBMP-2. Prior to surgery, the NZW rabbits were housed and fed in individual cages under the same condition for 7 days.

All rabbits underwent a cortical defect surgery in the distal femur (Ø 4.2 × 5 mm). The rabbits were anesthetized by intravenation injection via ear vein of 3% pentobarbital sodium at a dose of 3 mg/kg. After exposing the distal femur through a skin incision, the defect was created using a dental drill and rinsed with 0.9% saline to wash away remaining bone fragments. The bone defect was filled with a prepared cylinder scaffold. Following implantation, the wound was sutured and disinfectant was applied to the wound site to prevent infection. After the surgery, the rabbits were individually caged and fed. At week 4, 8 and 12, the rabbits underwent X-ray radiography examination to observe the regenerative process, and were sacrificed to obtain the bony specimens. All procedures were carried out following approval of Institutional Animal Care and Use Committee of National Tissue Engineering Center (Shanghai, China).

The retrieved bone specimens were prepared for histological analysis. The undecalcified sections were counter-stained with Van Gieson's picro fuchsin (VG) to observe the mineralized bone tissue microscopically. For hematoxylin/eosin (HE) staining, after fixation with 4% neutral buffered formalin, the specimens were decalcified in 12.5% EDTA, dehydrated in a graded series of alcohol, and embedded in paraffin. 4 μm thick sections were sliced, stained with HE and observed microscopically.

Pilot clinical trial

The clinical application of CPC/rhBMP-2 microffolds was approved by China Food and Drug Administration (CFDA Certified No. (2013): 34-60199); clinical protocols were approved by the respective ethic committees; and all patients gave informed consent before joining the study.

Patient selection

81 bone defect patients were enrolled in 3 hospitals in China, including the Sixth People's Hospital of Shanghai Jiao Tong University, Ninth People's Hospital of Shanghai Jiao Tong University, and Zhongshan Hospital of Shanghai. Details of surgical inclusion criteria are described below:

1. Age 16~70 years; 2. Tibial plateau fractures, proximal humeral fractures, or calcaneal fractures at a similar level of severity, of which the situation involves collapse and requires implantation; 3. An understanding of the rehabilitation protocol and willing to follow it; 4. An agreement to postoperative visits and tests; 5. Signed an informed subject consent form.

The patients were randomly divided into two groups and treated by CPC/rhBMP-2 microffolds or traditional CPC paste (control group).

Surgical procedure

All operations were done by doctors titled with associate chief physician or above. Procedures were performed under general anesthesia in a tertiary care medical center.

A minimally invasive internal fixation method had been applied in the surgeries. In brief, the patients with fracture were first treated by reduction of fracture, correction of displacement and deformity, and metal implant fixation. Then the collapse of the cancellous bone was filled with CPC/rhBMP-2 microffolds or CPC paste (product of Shanghai Rebone Biomaterials Co., Ltd, following the manufacturer's instruction), which was compacted to prevent the material from filling into the joint cavity.

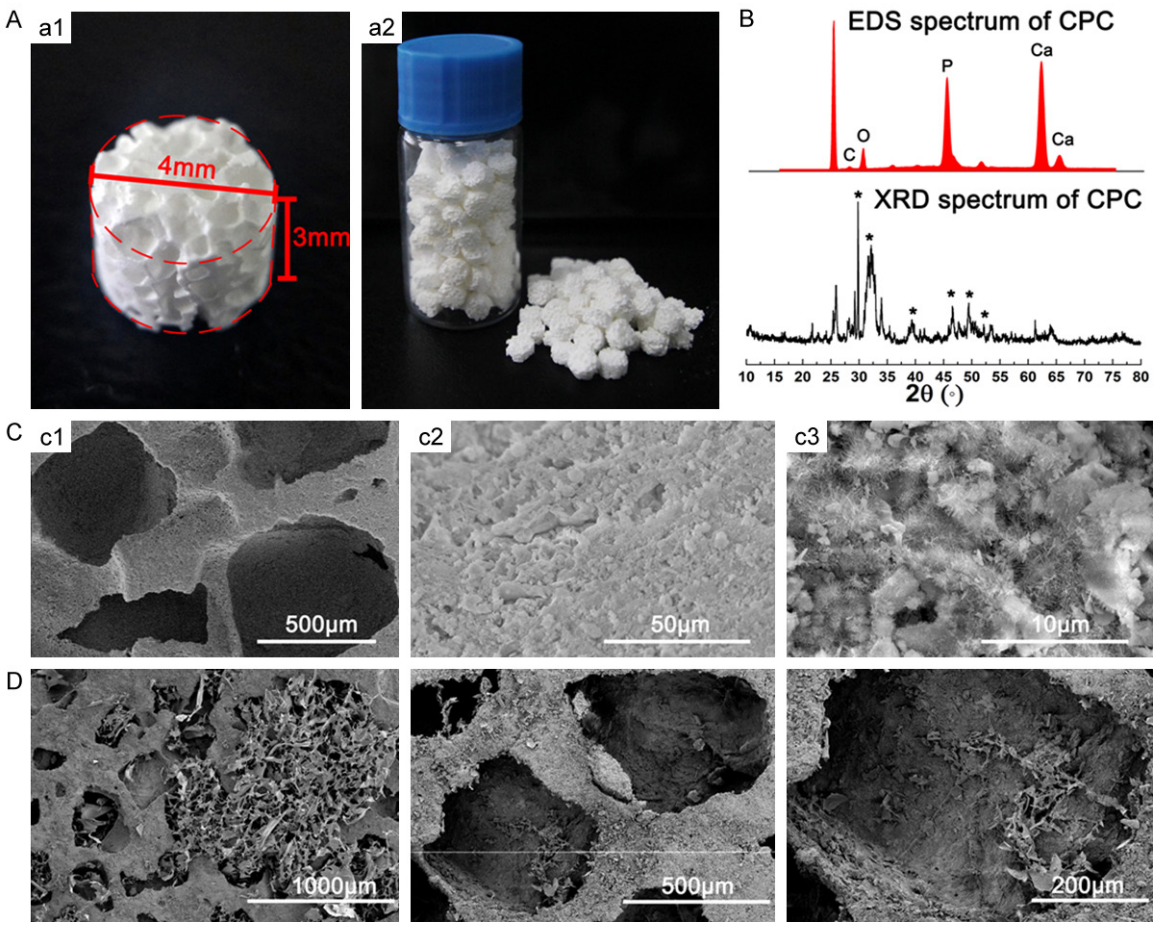

Figure 1. Physicochemical properties of CPC and CPC/rhBMP-2 micro-scaffolds: (A) Digital photographs of CPC/rhBMP-2 microffolds. (B) EDS and wide angle XRD spectra of CPC microffolds. Asterisks indicate specific peaks of hydroxyapatite: 28.2°, 32.8°, 39.7°, 46.6°, 49.5° and 52.1°. (C) SEM images of the interconnected macroporous (c1) and microporous structures (c2) of CPC microffolds, and crystal morphology of the surface hydroxyapatite (c3). (D) The immobilized protein adsorbed on the macroporous surface of CPC/rhBMP-2 microffolds.

X-ray imaging and function scoring

Post-operative follow-ups were conducted, and the assessment was based on clinical examination and X-ray radiographic imaging. After the CPC implantation, all patients were observed according to the following indexes: allergic or toxic reactions, rash or high fever. X-ray radiography at different time intervals after implantation was employed to observe the osseointegration of the implanted microffolds to host bone and the degradation of the material.

The time of clinical healing and fracture reunion were determined by observation of facture lines together with other physical criteria as described below. Criteria of clinical healing: 1) no local tenderness, vertical percussion pain or abnormal movements; 2) the ability of (upper limbs) stretching forward and bearing 1 kg for up to one minute or (lower limbs) continuously walking on the ground without crutches for three minutes and no less than 30 steps. 3) X-ray films showing massive bone trabeculae crossing barely discernible fracture line. Criteria of fracture reunion: 1) meet the criteria of clinical healing; 2) X-ray films showing homogeneous bone structure and obliterated fracture lines [29].

The functional recovery was recorded at each follow-up time point using IOWA knee and ankle score [30] in cases of tibial plateau and calcaneal fractures, and Neer shoulder score [31] in cases of proximal humeral fractures. The IOWA knee and ankle score is a questionnaire and clinical-examination-based evaluation of the function of the knee and ankle. The knee score is a five- category measurement, which includes activities of daily living, freedom from pain, gait,

aid dependence, deformity and range of movement. The ankle score is a four-category measurement of function, freedom from pain, gait and range of movement. Neer shoulder score has three parts: scoring of pain during the previous week by patients (verbal rating scale); clinical testing of function (muscle strength, reaching ability, and stability) and active range of motion; and an anatomical or radiological evaluation. Both IOWA and Neer scores are grouped into excellent (90 to 100), good (80 to 89), fair (70 to 79) and poor (under 70) categories.

Results

Microffolds designment and physicochemical properties

The CPC microffolds were designed to fill defect sites of different sizes and shapes with easy operability and sufficient macroporosities for tissue ingrowth (**Scheme 1A**). By a salt leaching and molding method, cylindrical CPC microffolds (Ø 4 mm × 3 mm, **Figure 1A**) were massively prepared. The microffolds were then sterilized, immobilized with rhBMP-2 by an adsorption and lyophilization process to achieve the final CPC/rhBMP-2 microffolds, which can be preserved for a long term and is easy to operate during surgeries (**Scheme 1A**).

The pre-cured CPC microffolds exhibited a composition of hydroxyapatite with low crystallinity (**Figure 1B**), which is similar to the inorganic phase of natural bone tissue. As shown in **Figure 1C**, the CPC microffolds exhibited interconnected macropores (c1) formed by NaCl granules and micropores (c2) formed by the saturated NaCl solution used in the formulation. The former ensured the ingrowth of cells and tissues as well as a rapid degradation of material, and the later enhanced the bioactivity of the scaffold and provided a high surface area for rhBMP-2 immobilization. Under a higher magnification (**Figure 1C**, c3), extensive needle-like hydroxyapatite crystals were observed in the surface of the microffold. As shown in **Figure 1D**, after rhBMP-2 immobilization, flocculent proteins was uniformly adsorbed on the macroporous surface of CPC/rhBMP-2 microffold.

Cytocompatibility, protein release kinetics and osteogenic capacity in vitro

In accordance with numerous previous researches that demonstrated the excellent cytocompatibility of CPC, the *in vitro* experiment data here indicated that rBMSCs had tightly anchored and well spread on both CPC and CPC/rhBMP-2 microffolds (**Figure 2A**), and the microffolds exerted no toxicity on cell proliferation compared to blank control (**Figure 2B**).

As indicated by the release curve of CPC/rhBMP-2 microffolds (**Figure 2C**), the profile exhibited a typical two-stage releasing kinetic: an initial burst occurring during the first 24 h and a slow sustained release during the rest of the time course. CD spectra of microffold-released rhBMP-2 and free rhBMP-2 (**Figure 2C** insert) and the structural analyses (**Table 1**) demonstrated that the secondary structure of microffold-released rhBMP-2 was well maintained (with only 5.69% structural change), which should be attributed to the gentle immobilization process mainly based on physical adsorption. The binding efficiency between rhBMP-2 and its receptor was detected by immunofluorescence staining of anti-BMP-2 primary antibody and FITC-conjugated goat-anti-mouse IgG. As intuitively shown in **Figure 2D**, the microffold-released rhBMP-2 exhibited an equal binding amount to that of free rhBMP-2, and thus led to an equivalent osteogenic efficiency as reconfirmed by ALP activity tests (**Figure 2E**). As shown in osteogenetic genes expression results (**Figure 2F**), CPC microffolds exhibited very limited osteoinductivity, which was significantly enhanced by the incorporation of rhBMP-2.

Rabbit distal femur defect repair

To evaluate the osteogenic performance of CPC/rhBMP-2 microffolds more deeply, rabbit distal femur defect repair experiments were conducted using CPC and CPC/rhBMP-2 scaffold with corresponding size and shape. All experimental rabbits exhibited no sign of wound infection. After the surgery, the incisions healed at week 1, and after 4 weeks the mobility of the operative limbs recovered to a normal level. As shown in **Figure 3**, the regenerative process was characterized by X-ray imaging (**Figure 3A**), VG (**Figure 3B**) and HE (**Figure 3C**) staining histological analyses.

At week 4 post-implantation, the boundary between bone tissue and CPC/rhBMP-2 scaffold became fuzzy to the naked eye, as the material and bone tissue started to integrate. As the shadow of X-ray imaging indicated, part

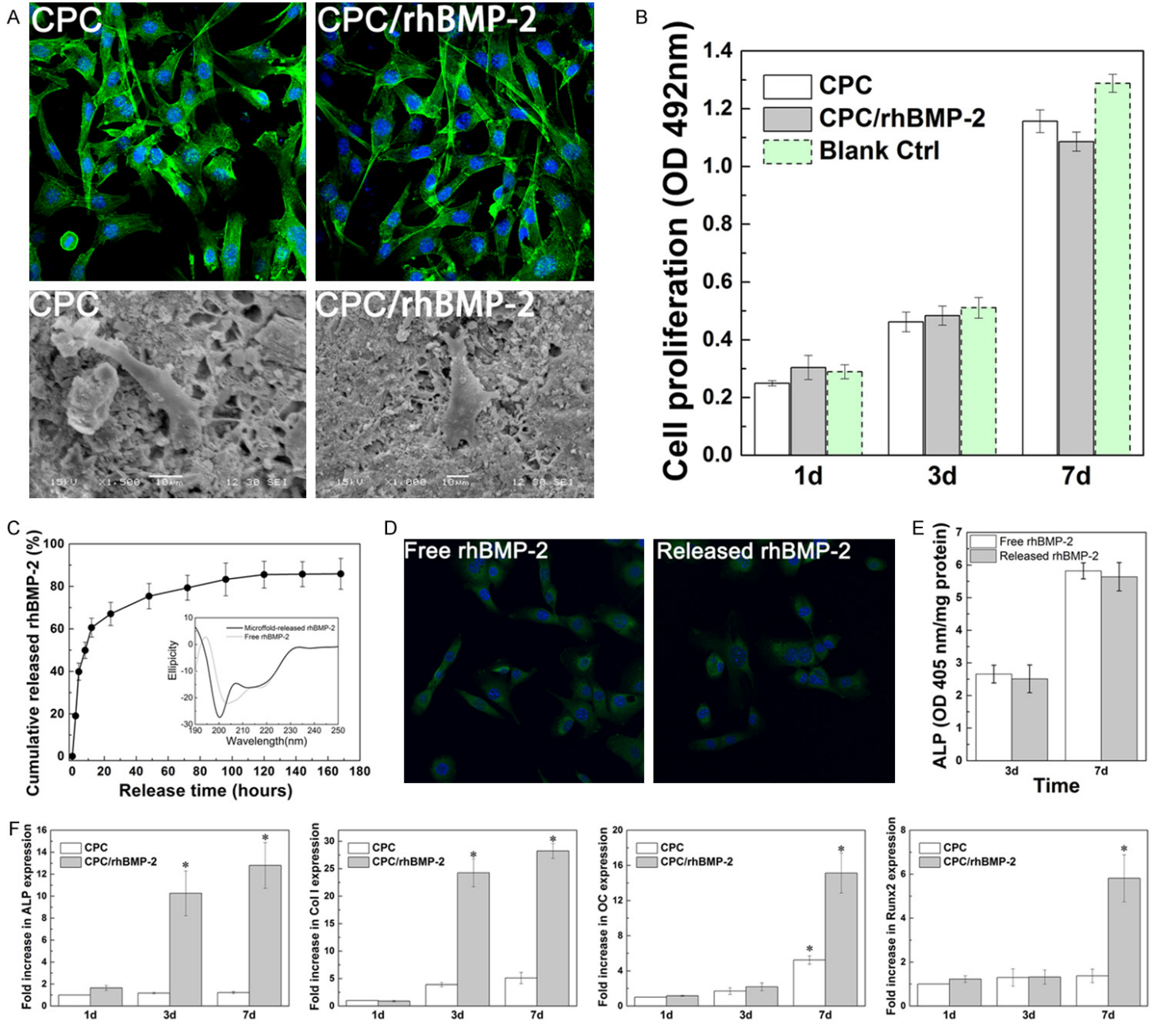
A
CPC
CPC/rhBMP-2
CPC
CPC/rhBMP-2
B
Cell proliferation (OD 492nm)
CPC
CPC/rhBMP-2
Blank Ctrl
1d
3d
7d
C
Cumulative released rhBMP-2 (%)
Release time (hours)
Microfold-released rhBMP-2
Free rhBMP-2
Ellipicity
Wavelength(nm)
D
Free rhBMP-2
Released rhBMP-2
E
ALP (OD 405 nm/mg protein)
Free rhBMP-2
Released rhBMP-2
Time
F
Fold increase in ALP expression
Fold increase in Col I expression
Fold increase in OC expression
Fold increase in Runx2 expression
CPC
CPC/rhBMP-2

Figure 2. *In vitro* evaluation of CPC and CPC/rhBMP-2 scaffolds: A. Morphological observation of rBMSCs attachment by SEM and cytoskeletal staining by CLSM on CPC and CPC/rhBMP-2 microffolds. B. Proliferation of rBMSCs cultured with CPC and CPC/rhBMP-2 microffolds. C. RhBMP-2 release profile of CPC/rhBMP-2 microffolds and CD spectra of microffold-released rhBMP-2 and free rhBMP-2 (insert). D. Observation of microffold-released rhBMP-2 and free rhBMP-2 bound on rBMSCs, detected by anti-BMP-2 antibody and FITC labeled anti-mouse IgG (green), with cell nuclei stained by DAPI (blue). E. ALP activity of microffold-released rhBMP-2 and free rhBMP-2. F. Osteogenetic genes (ALP, Col I, OC, Runx2) expression of rBMSCs on CPC and CPC/rhBMP-2 microffolds.

of the bone defect area had a density close to the host bone. While in contrast, in the groups of CPC scaffolds without rhBMP-2, edge of bone defect was relatively distinct at week 4, and the biodegradation of the implant material was not obvious. VG staining images exhibited red-stained woven bone surrounding the material and occupying the porosities in both groups, where CPC/rhBMP-2 microffold induced more continuous and more amount of bone tissue, and showed a fuzzier boundary. At week 8, it could be seen with naked eye that CPC/rhBMP-2 scaffold was tightly integrated with bone tissue, with extensive cartilage formation around the scaffold at the defect site. A significantly reduced shadow area was shown in the X-ray image, indicating that most of the scaffold were biodegraded and replaced by newly formed bone. The bone density of defect area was basically similar to the host bone, except a deeper shadow (higher density) in the center of the defect site where a small residual of the scaffold remained. The edge of pure CPC scaffold started to blur at week 8, indicating a gradual biodegradation of the material. VG staining indicated gradual degradation of material accompanied with new bone formation in both groups, and the rate of which in CPC group was much lower than in CPC/rhBMP-2 group. 12 weeks after implantation, regeneration of the bone defect was basically completed in CPC/rhBMP-2 group, with a faded shadow of the scaffold in X-ray image. The density of the newly formed bone at the defect site was close to the surrounded normal tissue. And at this time, in pure CPC scaffold group, a tight integration of scaffold and bone tissue with cartilage formation around the scaffold and gradual degradation of material was observed. Small residuals of CPC/rhBMP-2 microffold wrapped in bone tissue could be observed in VG staining images, while large parts of pure CPC microffold remained undegraded.

An endochondral bone formation process was intuitively revealed by HE staining histological analyses as shown in **Figure 3C**. In CPC/rhBMP-2 group, the defect site was filled by plenty of chondrocytes and newly formed cartilage at week 4, which gradually transformed into woven bone at week 8, followed by further mineralization into lamellar bone and formation of the medullary cavity. At week 12, completely degradation of material, maturely mineralized lamellar bone with typical ring-like Haversian osteons and blood vessels, and a matured bone marrow cavity with medulla ossium flava and medulla ossium rubra were achieved. In contrast, a similar regeneration process was observed in the pure CPC scaffold group, yet the rate of both tissue formation and material degradation was much lower.

Pilot clinical study and tissue imaging

The animal model provided some evidence of the osteogenic performance of microffolds in an active environment. However, clinically relevant defects in humans are substantially larger and more complicated than those that can be created in animal models. Therefore, the application of CPC/rhBMP-2 microffolds was evaluated in human bone defects. Patient demographics and clinicopathologies were shown in **Table 3**.

81 bone defect patients were randomly divided into two groups and treated by CPC/rhBMP-2 microffolds or traditional CPC paste (control group). In the CPC/rhBMP-2 group, 40 patients included 25 males and 15 females, with an average age of 46.7; the bone defects were located as follows: tibial plateau in 16 patients, proximal humerus in 11 patients and calcaneus in 13 patients; the defects were repaired with CPC/rhBMP-2 microffolds. In the control group, 41 patients included 27 males and 14 females, with an average age of 44.3; the bone defects were located as follows: tibial plateau in 15 patients, proximal humerus in 12 patients and calcaneus in 14 patients; the defects were repaired with traditional CPC paste.

7~12 days post-operation, skin wound healing by first intention of the surgical incisions was acquired in 78 cases; wound exudation occurred in 1 case of control group and 2 cases of

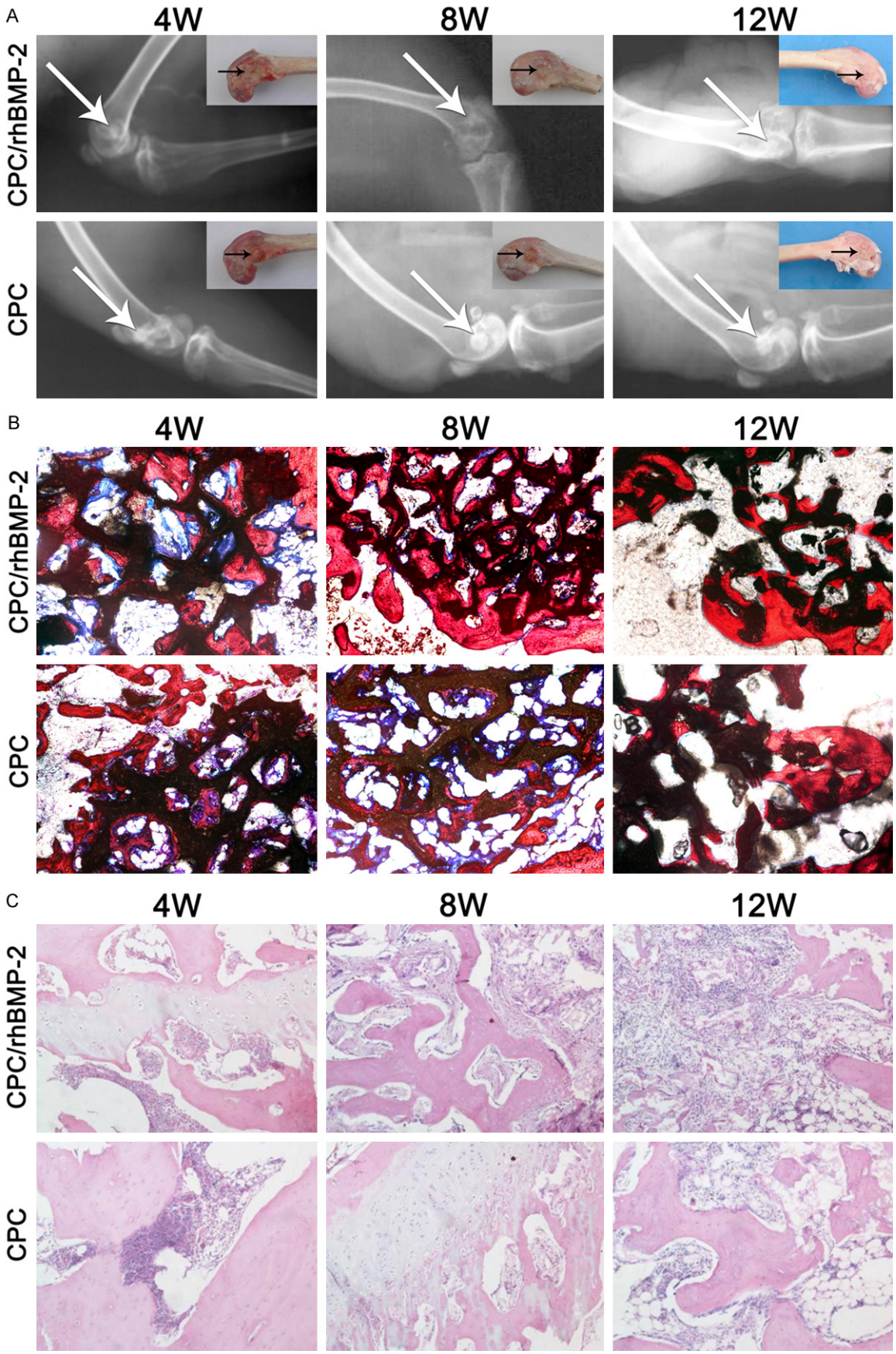
A
4W
8W
12W
CPC/rhBMP-2
CPC
B
4W
8W
12W
CPC/rhBMP-2
CPC
C
4W
8W
12W
CPC/rhBMP-2
CPC

Figure 3. *In vivo* evaluation of bone formation by CPC and CPC/rhBMP-2 scaffolds in a rabbit distal femur defect model: (A) X-ray imaging and tissue observation (insert), histological analyses by (B) VG and (C) HE staining at week 4, 8 and 12.

Table 3. Patient demographics and clinicopathologies. A total of 81 patients were evaluated

Groups	Patient information				Bone defect site		
	Number of patients	Age range	Average age		Tibial plateau	Proximal humerus	Calcaneus
Traditional CPC paste	M27, F14	16-70	44.3	Number of patients	15	12	14
				Wound exudation	1	0	0
				Toxic effect, skin rash or high fever	0	0	0
				Average time of clinical healing (months)	4.6	2.6	3.1
				Average time of bony reunion (months)	6.5	3.5	4.7
CPC/rhBMP-2 microffolds	M25, F15	16-70	46.7	Number of patients	16	11	13
				Wound exudation	2	0	0
				Toxic effect, skin rash or high fever	0	0	0
				Average time of clinical healing (months)	3.5	2	2.4
				Average time of bony reunion (months)	4.3	2.7	3.5

CPC/rhBMP-2 group 2 weeks post-operation, which were all healed after dressing change. These implant rejections were diagnosed as idiopathic non-infectious inflammatory, which might be related with blood supply deficiency, scar constitution, long time of limb fixation, or heterologous protein allergy. No toxic effect, skin rash or high fever was found in all patients; liver and kidney functions, routine blood and urine tests and C-reactive protein were normal. All cases were followed up for 12~24 months, average 15.3 months. During follow-up, no occurrence of osteomyelitis, fractures, or obvious collapses after the bone defect repair was observed; no plate and screw loosening or other complications occurred. The average time of clinical healing and bony reunion by CPC/rhBMP-2 microffolds was significantly shortened compared to the control group repaired by traditional CPC paste (**Table 3**); and the average function scores and the excellent rates of function scores at each time point also indicated shortened repairing time and higher repairing qualities in CPC/rhBMP-2 microffolds group (**Table 4**).

Typical cases were selected and shown in **Figures 4**, **5**, including 3 cases of tibial plateau fractures, 3 cases of proximal humeral fractures and 1 case of calcaneal fracture. The X-ray films intuitively indicated the acceleration of clinical healing (red dashed arrows) and bony reunion (red dashed circles) by CPC/rhBMP-2 microffolds. Take the typical cases of tibial plateau fractures as examples (**Figure 4**), 1 month post-operation, the anatomic shapes of the bone defects were all recovered after surgery; bone filler materials were closely connected with the host bone; there was no gap between the bone and the filling material at the interface; and facture lines were clearly visible in both groups. In the cases using CPC/rhBMP-2 microffolds (**Figure 4**, Case 1-1 and 1-2), the fracture lines became fuzzy at month 2, progressively faded and total disappeared at week 4. The fuzziness of facture lines together with other physical criteria (see Materials and methods section) was considered as clinical healing, and the disappearance of fracture line was considered as bony reunion. In contrast, in case of traditional CPC paste (**Figure 4**, Comparable Case 1), the time of clinical healing and bony reunion were postponed to month 4 and month 8. Moreover, CPC/rhBMP-2 microffolds exhibited a similar density to the host bone due to its abundant porous structure, while traditional CPC paste showed a white shadow indicating high density, which results from slow degradation and clear vision of the material remained after bony reunion. Similar trends could be observed from the typical cases of proximal humeral fractures and calcaneal fracture (**Figure 5**).

Furthermore, we had accepted two additional cases that could not be treated successfully by traditional treatment (**Figure 6**). Additional Case A was a male patient of 26, bone nonunion of phalangeal fractures after internal fixation and treated with tradition CPC paste filling therapy, implanted CPC/rhBMP-2 microffolds in revision. The X-ray films exhibited gradual degra-

Table 4. Statistics of functional scores of patients, applying IOWA knee and ankle score in cases of tibial plateau and calcaneal fractures, and Neer shoulder score in cases of proximal humeral fractures

Defect site/score system	Group	Time point									
		3 months		4 months		6 months		8 months		12 months	
		Average score	Excellent and good rate	Average score	Excellent and good rate	Average score	Excellent and good rate	Average score	Excellent and good rate	Average score	Excellent and good rate
Tibial plateau (IOWA score)	Traditional CPC paste	64.8 ± 7.9	5%	80.3 ± 5.8	50%	83.8 ± 5.7	75%	85.2 ± 4.8	85%	88.6 ± 4.5	90%
	CPC/rhBMP-2 microffolds	75.3 ± 8.5	25%	84.7 ± 4.0	88%	88.3 ± 5.2	94%	93.9 ± 3.7	100%	95.6 ± 3.2	100%
Proximal humerus (Neer score)	Traditional CPC paste	77.4 ± 8.2	38%	80.4 ± 4.3	75%	87.5 ± 5.2	100%	-	-	-	-
	CPC/rhBMP-2 microffolds	83.5 ± 7.3	57%	90.6 ± 5.4	100%	96.2 ± 2.8	100%	-	-	-	-
Calcaneus (IOWA score)	Traditional CPC paste	50.7 ± 10.2	0%	78.5 ± 7.3	42%	82.9 ± 4.2	84%	83.6 ± 3.5	89%	-	-
	CPC/rhBMP-2 microffolds	62.4 ± 11.9	9%	80.6 ± 6.4	64%	85.4 ± 5.0	95%	91.0 ± 3.2	100%	-	-

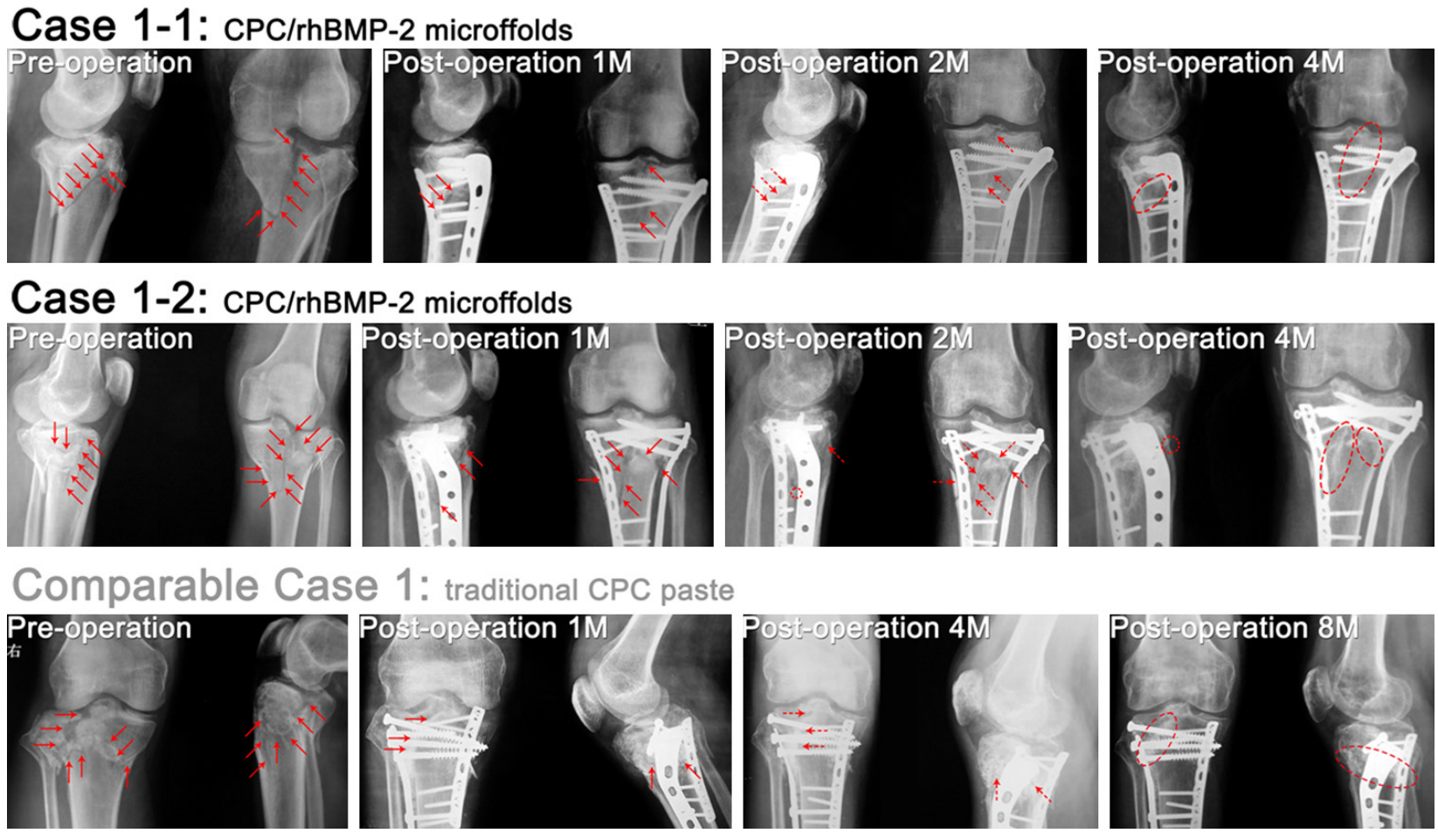

Figure 4. Typical cases of tibial plateau fractures: two cases (Case 1-1 and Case 1-2) repaired by CPC/rhBMP-2 microffolds, and a comparable case (Comparable Case 1) repaired by traditional CPC paste. Red solid arrows indicate the fracture lines; red dashed arrows indicate fuzzy fracture lines, which were considered as clinical healing; red dashed circles indicate the disappearance of the fracture lines, which was considered as bony reunion.

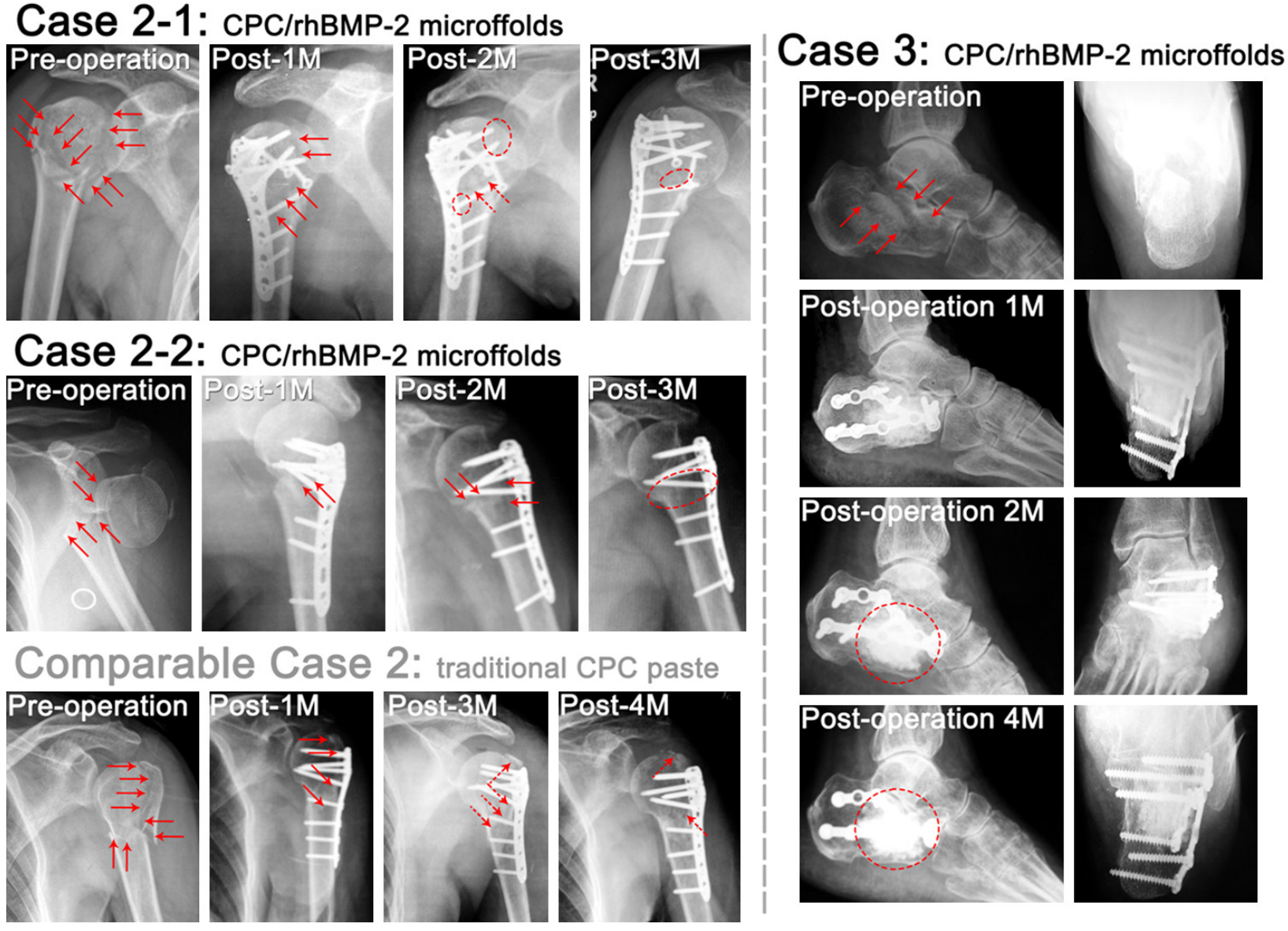

Figure 5. Left: Typical cases of proximal humeral fractures: two cases (Case 2-1 and Case 2-2) repaired by CPC/rhBMP-2 microffolds and a comparable case (Comparable Case 2) repaired by traditional CPC paste. Right: Typical case of calcaneal fracture (Case 3) repaired by CPC/rhBMP-2 microffolds. Red solid arrows indicate

the fracture lines; red dashed arrows indicate fuzzy fracture lines, which were considered as clinical healing; red dashed circles indicate the disappearance of the fracture lines, which was considered as bony reunion.

dation of material accompanied with trabecular bone ingrowth after 1 month; after 6 months, the microffolds were replaced by host bone tissue and clinical healing was achieved; after the removal of internal fixation 9 months post-operation, the affected finger was healed with complete bony reunion. Additional Case B was a 17-year-old male patient of scoliosis, who received orthopedic surgery of intervertebral fusion and pedicle screw fixation, using CPC/rhBMP-2 microffolds in left side and autografts in right side, respectively. The orthopedic outcome 12 months post-operation was satisfactory with internal fixation in place. After removal of internal fixation 19 months post-operation, the X-ray films exhibited obvious callus formation in the side of CPC/rhBMP-2 microffolds (red dashed circle), and no callus formation in the side of autografts (green dashed circle), indicating a better therapeutic efficacy of CPC/rhBMP-2 microffolds than autografts.

These results demonstrated that CPC/rhBMP-2 microffolds were superior to traditional CPC paste in overall performances, with not only shortened repairing time, but also improved repairing qualities. Moreover, CPC/rhBMP-2 microffolds exhibited the potential in treating fractures that are most challenging for current therapies.

Discussion

Despite that the great potential of porous scaffolds and growth factors in the field of bone repairing has been well-acknowledged, most porous scaffolds are still in developmental stages, and most growth factors have very limited clinical application due to the lack of proper carriers and an unaffordable cost.

Currently, scaffolds of specific size and shape can be prepared according to the protocol of the selected animal model, for example, long cylinder-shaped scaffolds for radius defect models [32], oblate scaffolds for cranial defect models [33], etc. However, bone defects of clinical patients come in various sizes and shapes, which cannot be accurately determined with current imaging techniques, and the duration from the occurrence of defect to surgical treatment is too short to order and customize the scaffolds (**Scheme 1A**, traditional scaffolds). The concept of "microffolds" proposed in this study could provide a trajectory to the clinical translation of porous scaffolds. The microffolds were designed not only to retain the advantageous macroporosities of traditional scaffolds, but also for a better operability that is not restricted to the defect size and shape, which avoids the needs of customization, and allows massive production and long-term preservation in advance (**Scheme 1A**, microffolds).

Traditional CPC paste currently used in clinic has a porosity of 30~60% with pore size of ~1 μm due to its inherent physicochemical properties, however, these pores are too small to allow fast bone ingrowth and CPC bioresorbs layer by layer slowly *in vivo* (**Scheme 1B**, traditional CPC). Traditional CPC paste can be filled into different sized and shaped defect site, however, due to its high density, the material cannot degrade completely and be replaced by new bone until years later in most patients' cases, which makes this feature the main drawback of CPC. Preparation of CPC into porous scaffolds can effectively solve this drawback. In this study, the abundant macroporous and microporous structures (**Figure 1C**), similar composition to that of natural bone (**Figure 1B**), and the inherent excellent biocompatibility of CPC (**Figure 2**) had endowed the CPC microffolds with biodegradability and excellent osteoconductivity (**Figure 3**). Compared to traditional CPC paste, the macroporosities of CPC microffolds ensured rapid ingrowth of tissue and synchronous material degradation (**Scheme 1B**), which lead to an accelerated regeneration in clinic (**Figures 3**, **4**).

The introduction of rhBMP-2 has greatly accelerated new bone formation and material degradation *in vivo* (**Figure 3**). Current rhBMP-2 productions for clinical use mainly adopted hydrogel as carrier, however, since hydrogels lacked osteoconductivity and controlled release, high doses of rhBMP-2 were required to achieve desirable osteogenic efficiency, which had raised the cost to an unaffordable level. In addition, since current artificial bone substitutes (for example, traditional CPC paste) exhibited no notable advantage in the repairing efficiency comparing to autografts, most patients would

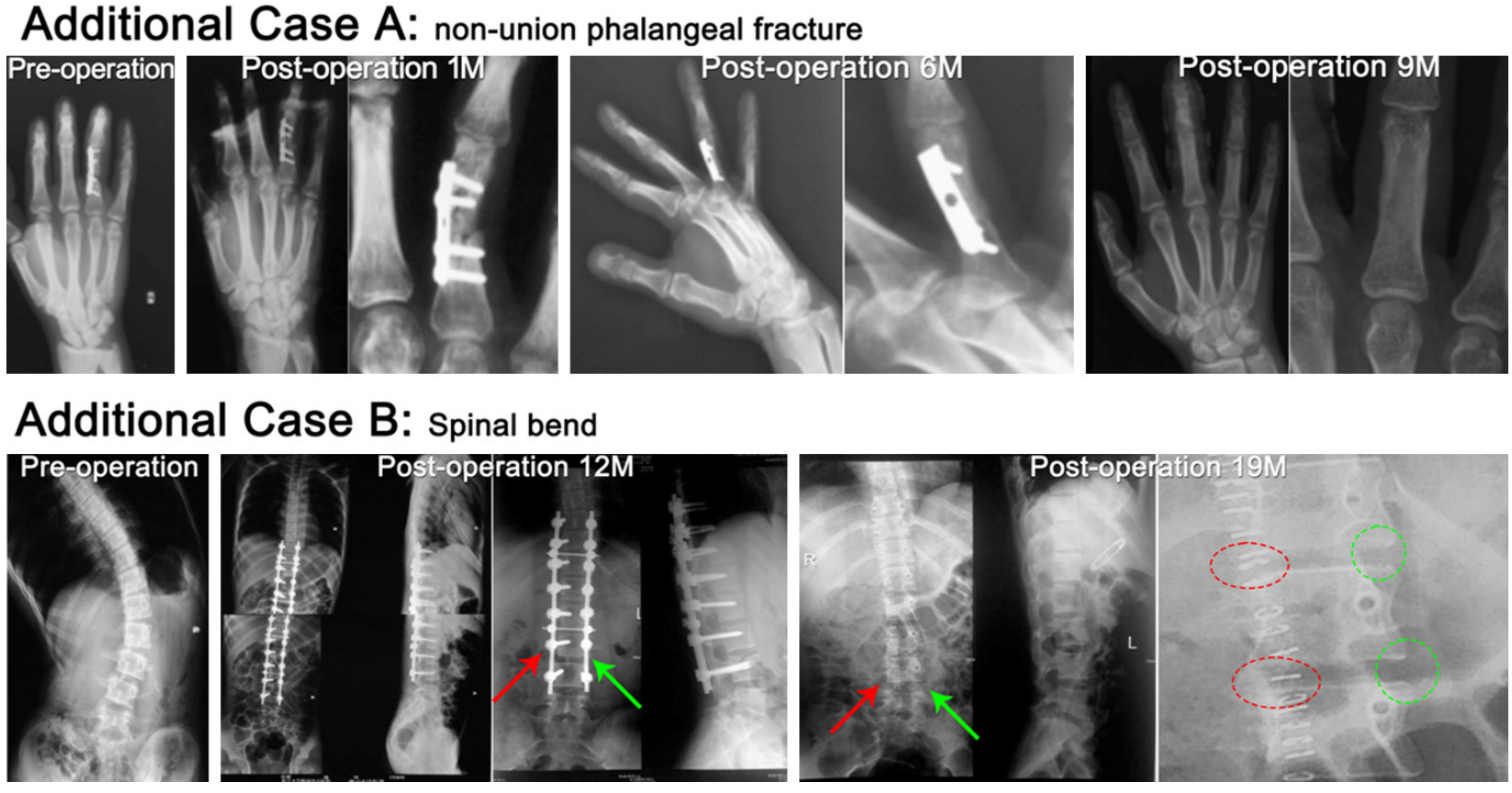

Figure 6. Two additional cases: non-union phalangeal fracture (Additional Case A) repaired by CPC/rhBMP-2 microffolds and scoliosis (Additional Case B) implanted with CPC/rhBMP-2 microffolds and autografts. Additional Case B applies CPC/rhBMP-2 microffolds (red arrow) and allografts (green arrow) to each side of the spine; red dashed circle indicated callus formation on the side of CPC/rhBMP-2 microffolds, while green dashed circle exhibited no callus formation on the side of allografts.

rather choose autografts for its relatively low cost and high efficiency [34]. As a solvation and improvement to current substitutes, the CPC/rhBMP-2 microffolds combined the osteoconductivity of porous CPC scaffolds and the osteoinductivity of rhBMP-2, and thus achieved a rapid bone repair with relatively low dose of rhBMP-2. Compared to current clinical therapies (traditional CPC paste), the average fracture healing time was 0.5~2 months shorter after implanted CPC/rhBMP-2 microffolds (**Table 3**), and the defect site could rapidly recover to a satisfactory functional level 3-6 months post-implantation (**Table 4**). Moreover, CPC/rhBMP-2 microffolds exhibited the potential in treating fractures that are most challenging for current therapies (**Figure 6**).

In conclusion, by combining two mature clinical applications of material and growth factor, CPC and rhBMP-2, we for the first time brought bone substitutes based on scaffold/growth factor to clinical trials, and provided data support for clinical translation of this area. The concept of "microffold" proposed in this study, could be extended to the clinical translation of porous scaffolds of various materials. The CPC/rhBMP-2 microffold developed in this study is expected to be widely applied in clinical, and provide more effective therapeutic treatment for bone repair.

Acknowledgements

This work was supported by grants from the National Basic Research Program of China (973 Program, No. 2012CB933600), the 111 Project (B14018), the National Natural Science Foundation of China (No. 31330028 and 31470924). The pilot clinical trial of CPC/rhBMP-2 microffolds as bone substitute for bone regeneration has been registered at clinicaltrials.gov (ID: NCT02609074).

Abbreviations

CPC, Calcium phosphate cement; rhBMP-2, Recombinant human bone morphogenetic protein-2; PBS, Phosphate buffer solution.

Address correspondence to: Yuan Yuan, The State Key Laboratory of Bioreactor Engineering, East China University of Science and Technology, Box 112, No. 130, Meilong Road, Shanghai 200237, P.R. China. Tel: +86-21-64251308; Fax: +86-21-6425-1358; E-mail: yyuan@ecust.edu.cn; Jinwu Wang, Department of Orthopaedic Surgery, Ninth People's Hospital of Shanghai Jiao Tong University, Room 703, Building 3, No. 639, Zhizaoju Road, Shanghai 200011, P.R. China. Tel: +86-21-55151786; Fax: +86-21-63139920; E-mail: jinwu_wang@163.com; Changsheng Liu, The State Key Laboratory of Bioreactor Engineering; Key Laboratory for Ultrafine Materials of Ministry of Education; Engineering Research Center for Biomedical Materials of Ministry of Education, East China University of Science and Technology, Box 112, No. 130, Meilong Road, Shanghai 200237, P.R. China. Tel: +86-21-6425-1358; Fax: +86-21-64251358; E-mail: liucs@ecust.edu.cn

References

[1] Yuan H, Fernandes H, Habibovic P, de Boer J, Barradas AM, de Ruiter A, Walsh WR, van Blitterswijk CA, de Bruijn JD. Osteoinductive ceramics as a synthetic alternative to autologous bone grafting. Proc Natl Acad Sci U S A 2010; 107: 13614-9.

[2] Tagil M. Bone Substitutes, Grafts and Cement. In: Hove LM, Lindau T, Hølmer P, editors. Distal Radius Fractures: Springer Berlin Heidelberg; 2014. pp. 233-9.

[3] Smith CA, Richardson SM, Eagle MJ, Rooney P, Board T, Hoyland JA. The use of a novel bone allograft wash process to generate a biocompatible, mechanically stable and osteoinductive biological scaffold for use in bone tissue engineering. J Tissue Eng Regen Med 2015; 9: 595-604.

[4] Dumic-Cule I, Pecina M, Jelic M, Jankolija M, Popek I, Grgurevic L, Vukicevic S. Biological aspects of segmental bone defects management. Int Orthop 2015; 39: 1005-11.

[5] Aponte-Tinao L, Ayerza M, Muscolo DL, Farfalli G. What Are the Risk Factors and Management Options for Infection After Reconstruction With Massive Bone Allografts? Clin Orthop Relat Res 2015: 1-5.

[6] Lee IH, Chung CY, Lee KM, Kwon SS, Moon SY, Jung KJ, Chung MK, Park MS. Incidence and Risk Factors of Allograft Bone Failure After Calcaneal Lengthening. Clin Orthop Relat Res 2015; 473: 1765-74.

[7] Yunus Basha R, Sampath Kumar TS, Doble M. Design of biocomposite materials for bone tissue regeneration. Mater Sci Eng C Mater Biol Appl 2015; 57: 452-63.

[8] Tian B, Liu J, Dvir T, Jin L, Tsui JH, Qing Q, Suo Z, Langer R, Kohane DS, Lieber CM. Macroporous nanowire nanoelectronic scaffolds for synthetic tissues. Nat Mater 2012; 11: 986-94.

[9] Kraehenbuehl TP, Langer R, Ferreira LS. Three-dimensional biomaterials for the study of human pluripotent stem cells. Nat Methods 2011; 8: 731-6.
[10] Cancedda R, Giannoni P, Mastrogiacomo M. A tissue engineering approach to bone repair in large animal models and in clinical practice. Biomaterials 2007; 28: 4240-50.
[11] Shayesteh YS, Khojasteh A, Soleimani M, Alikhasi M, Khoshzaban A, Ahmadbeigi N. Sinus augmentation using human mesenchymal stem cells loaded into a β-tricalcium phosphate/hydroxyapatite scaffold. Oral Surg Oral Med Oral Pathol Oral Radiol Endod 2008; 106: 203-9.
[12] Kokemueller H, Spalthoff S, Nolff M, Tavassol F, Essig H, Stuehmer C, Bormann KH, Rücker M, Gellrich NC. Prefabrication of vascularized bioartificial bone grafts in vivo for segmental mandibular reconstruction: experimental pilot study in sheep and first clinical application. Int J Oral Maxillofac Surg 2010; 39: 379-87.
[13] Vallet-Regi M, Ruiz-Hernandez E. Bioceramics: From Bone Regeneration to Cancer Nanomedicine. Adv Mater 2011; 23: 5177-218.
[14] Anderson JM, Patterson JL, Vines JB, Javed A, Gilbert SR, Jun HW. Biphasic Peptide Amphiphile Nanomatrix Embedded with Hydroxyapatite Nanoparticles for Stimulated Osteoinductive Response. Acs Nano 2011; 5: 9463-79.
[15] Facca S, Cortez C, Mendoza-Palomares C, Messadeq N, Dierich A, Johnston AP, Mainard D, Voegel JC, Caruso F, Benkirane-Jessel N. Active multilayered capsules for in vivo bone formation. Proc Natl Acad Sci U S A 2010; 107: 3406-11.
[16] Schindeler A, McDonald MM, Bokko P, Little DG. Bone remodeling during fracture repair: The cellular picture. Semin Cell Dev Biol 2008; 19: 459-66.
[17] Hunziker EB, Enggist L, Kuffer A, Buser D, Liu Y. Osseointegration: The slow delivery of BMP-2 enhances osteoinductivity. Bone 2012; 51: 98-106.
[18] Li L, Zhou G, Wang Y, Yang G, Ding S, Zhou S. Controlled dual delivery of BMP-2 and dexamethasone by nanoparticle-embedded electrospun nanofibers for the efficient repair of critical-sized rat calvarial defect. Biomaterials 2015; 37: 218-29.
[19] Bessa PC, Casal M, Reis RL. Bone morphogenetic proteins in tissue engineering: the road from laboratory to clinic, part II (BMP delivery). J Tissue Eng Regen Med 2008; 2: 81-96.
[20] Geiger M, Li RH, Friess W. Collagen sponges for bone regeneration with rhBMP-2. Adv Drug Deliv Rev 2003; 55: 1613-29.
[21] Hsu WK, Wang JC. The use of bone morphogenetic protein in spine fusion. Spine J 2008; 8: 419-25.
[22] Jonkheijm P, Weinrich D, Schroder H, Niemeyer CM, Waldmann H. Chemical Strategies for Generating Protein Biochips. Angew Chem-Int Edit 2008; 47: 9618-47.
[23] Lee JS, Suarez-Gonzalez D, Murphy WL. Mineral Coatings for Temporally Controlled Delivery of Multiple Proteins. Adv Mater 2011; 23: 4279-84.
[24] Shah NJ, Hyder MN, Moskowitz JS, Quadir MA, Morton SW, Seeherman HJ, Padera RF, Spector M, Hammond PT. Surface-Mediated Bone Tissue Morphogenesis from Tunable Nanolayered Implant Coatings. Sci Transl Med 2013; 5: 191ra83.
[25] Kim RY, Oh JH, Lee BS, Seo YK, Hwang SJ, Kim IS. The effect of dose on rhBMP-2 signaling, delivered via collagen sponge, on osteoclast activation and in vivo bone resorption. Biomaterials 2014; 35: 1869-81.
[26] Conde MC, Chisini LA, Demarco FF, Nör JE, Casagrande L, Tarquinio SB. Stem cell-based pulp tissue engineering: variables enrolled in translation from the bench to the bedside, a systematic review of literature. Int Endod J 2015; [Epub ahead of print].
[27] Bose S, Tarafder S. Calcium phosphate ceramic systems in growth factor and drug delivery for bone tissue engineering: a review. Acta Biomater 2012; 8: 1401-21.
[28] Pan W, Li D, Wei Y, Hu Y, Zhou L. Tendon-to-bone healing using an injectable calcium phosphate cement combined with bone xenograft/BMP composite. Biomaterials 2013; 34: 9926-36.
[29] Hammer RR, Hammerby S, Lindholm B. Accuracy of radiologic assessment of tibial shaft fracture union in humans. Clin Orthop Rel Res 1985: 233-8.
[30] Merchant TC, Dietz FR. Long-term follow-up after fractures of the tibial and fibular shafts. J Bone Joint Surg Am 1989; 71: 599-606.
[31] Neer CS. Displaced Proximal Humeral Fractures. J Bone Joint Surg Am 1970; 52: 1077-89.
[32] Jing Z, Huanjun Z, Kai Y, Yuan Y, Changsheng L. RhBMP-2-loaded calcium silicate/calcium phosphate cement scaffold with hierarchically porous structure for enhanced bone tissue regeneration. Biomaterials 2013; 34: 9381-92.
[33] Zhang J, Ma X, Lin D, Shi H, Yuan Y, Tang W, Zhou H, Guo H, Qian J, Liu C. Magnesium modification of a calcium phosphate cement alters bone marrow stromal cell behavior via an integrin-mediated mechanism. Biomaterials 2015; 53: 251-64.
[34] Zhang LG, Khademhosseini A, (Eds.) TW. Tissue and Organ Regeneration: Advances in Micro-and Nanotechnology: CRC Press; 2014.